Available online at www.sciencedirect.com
ScienceDirect
International Journal of Mass Spectrometry 266 (2007) 149–155
International Journal of Mass Spectrometry
www.elsevier.com/locate/ijms

# Photodissociation of iron-pyrene and iron-perylene cation complexes

A.C. Scott, J.W. Buchanan, N.D. Flynn, M.A. Duncan *

*Department of Chemistry, University of Georgia, Athens, GA 30602-2556, USA*

Received 16 June 2007; received in revised form 18 July 2007; accepted 18 July 2007
Available online 22 July 2007

**Abstract**

Gas-phase cation complexes between iron atoms and the polycyclic aromatic hydrocarbons (PAHs) pyrene ($C_{16}H_{10}$) and perylene ($C_{20}H_{12}$) are produced in a molecular beam using laser vaporization in a pulsed nozzle cluster source. Mass spectrometry reveals the formation of clusters of the form $Fe_x(pyrene)_y^+$ for up to $x=4$ and $y=2$ and $Fe_x(perylene)_y^+$ for up to $x=2$ and $y=3$. Photodissociation studies show that the PAH ligand molecular cation is the most prominent fragment for each system. In both systems, species with more than one iron present fragment by the loss of neutral iron atoms. Additionally, there is evidence that these clusters form sandwich and multi-metal sandwich structures.


*Keywords:* Organometallic ions; Photodissociation; Metal clusters

## 1. Introduction

Transition metal π complexes occupy a central position in organometallic chemistry, and new variations on these systems continue to be found [1]. In recent years, gas-phase synthetic methods have been applied to these systems, producing novel complexes with unusual aromatic ligands. Metal complexes with fullerenes [2–16] and polycyclic aromatic (PAH) species [17–26] have demonstrated fascinating structures, spectroscopy and photochemistry. For example, Martin and co-workers were able to produce metal-coated $C_{60}$ [2–8] using a variety of metals. Jarrold and co-workers found evidence for fullerenes with metal incorporated into the cage wall [16]. Even metal–benzene complexes, which are well known in conventional organometallic chemistry, have been found to demonstrate unusual structures and photochemistry in gas-phase systems [27–36]. Kaya and co-workers have reported multiple decker sandwiches for transition metal–benzene complexes [31–36], as well as those with $C_{60}$ [12–14] and ferrocene [37] acting as ligands. In related work, lanthanide metals were found to produce multiple decker sandwiches with cyclooctatetrene [38,39] or $C_{60}$ [15]. Our research group has also produced and studied a variety of complexes of transition metals with benzene [27–30], $C_{60}$ [9–11] and cyclooctatetrene [40,41]. Transition metal complexes with PAH species were first produced by Dunbar and co-workers [17,18], and more recently our group has described numerous examples of these systems [19–26]. In the present work, we extend these studies to include the production and photodissociation of iron-pyrene and iron-perylene cation clusters.

Metal-PAH clusters are interesting for a variety of reasons. PAHs are often used by theorists to represent a finite section of graphite to study surface physisorption dynamics and energetics. Moreover, these systems may be used to model metal attachment to the walls of carbon nanotubes or metal intercalated graphite. Additionally, metal-PAH complexes are thought to form in interstellar gas clouds and to contribute to the depletion of metal in these environments [42–45]. PAHs have been implicated as carriers of the unidentified infrared bands (UIBs) or diffuse interstellar bands (DIBs), which are observed in all parts of the galaxy [42–45]. Moreover, they are estimated to account for 5–15% of the cosmic carbon, which would make them a significant component of the interstellar medium. However, recent studies have shown that the spectra of PAHs alone do not match the astrophysical spectra. As a result, it is thought that various PAH complexes, including perhaps those with metal, may explain these UIBs and DIBs. Iron is one of the most abundant metals in these environments, and so iron-PAH species have attracted much attention.

Metal cluster ions with selected PAHs have been described previously. Dunbar and co-workers were the first to make metal-PAH systems in the gas-phase [17,18], using FT-ICR mass spectrometry to probe the association kinetics of var-

* Corresponding author.
*E-mail address:* maduncan@uga.edu (M.A. Duncan).

1387-3806/$ – see front matter © 2007 Elsevier B.V. All rights reserved.
doi:10.1016/j.ijms.2007.07.009

ious metal ions with coronene ($C_{24}H_{12}$; mass = 300 amu). Recently, Szczepanski et al. measured vibrational spectra of cationic iron complexes with benzene, naphthalene and fluorene [45]. Theorists have performed calculations to determine the binding configurations and energetics of various metals on different PAHs [46–48]. Our research group has produced and studied numerous metal-PAH systems with time-of-flight mass spectrometry and mass-selected laser photodissociation, such as iron-coronene [11,19], silver-coronene [20], chromium-coronene [22], and niobium with coronene and pyrene [23]. In each of these systems, multiple metal atoms were found to bind to a single PAH ring system. Additionally, multiple PAH ligands were incorporated into these clusters, with strong evidence for the formation of sandwich structures and some indication for the presence of sandwiches with multiple metal atom fillings. In the iron-coronene system, it was found that the metal binds to intact coronene molecules and that this system eliminates neutral iron atoms rather than molecular metal fragments as the cluster decomposes. However, in the chromium-coronene system, one of the fragmentation channels was the elimination of molecular chromium clusters (e.g., $Cr_3$) as opposed to the loss of individual atoms. In both of the studies with iron or chromium clustering on coronene, there appeared to be a "templating" effect, in which there was a preference for three metal atoms per PAH surface. In the present study, we investigate the clustering behavior of iron with pyrene ($C_{16}H_{10}$; mass = 202 amu) and perylene ($C_{20}H_{12}$; mass = 252 amu). In these smaller PAH systems, we explore possible metal templating effects, the nature of metal binding configurations (atomic versus clustered), as well as the tendency for sandwich formation.

## 2. Experimental

Clusters for these experiments are produced by laser vaporization in a pulsed nozzle source. The experimental apparatus has been described previously [9–11,19–24]. The specially prepared samples for these experiments are pure iron rods coated with a thin film of either pyrene or perylene. Because pyrene and perylene are solids at room temperature, they must be sublimed onto the iron rod. Films are deposited in a small vacuum chamber dedicated for sample preparation, which has been described previously [9–11,19–24]. Once the sample is prepared, it is transferred to the molecular beam machine. Laser vaporization of the film coated metal rod is accomplished using the third harmonic (355 nm) of a pulsed Nd:YAG laser. The conditions are similar to those described for metal-coronene complex formation, where signals are sensitive to both film thickness and the vaporization laser power [19–24]. Under optimized conditions, the vaporization laser desorbs the ligand and penetrates to ablate the underlying metal, thus producing both species in the gas-phase. Clusters grow by recombination in the gas channel, which extends beyond the vaporization point. The cation clusters produced directly in the source pass through a skimmer and are extracted from the molecular beam into the mass spectrometer with pulsed acceleration voltages.

Mass-selected photodissociation experiments take place in the same reflectron time-of-flight mass spectrometer with the activation of a pulsed deflection plate (the "mass-gate"), which allows size selection of certain cluster masses. The operation of the instrument for these experiments has been described previously [9–11,19–24,27,30]. The time-of-flight through an initial drift tube section is used to size select the desired cluster, which is then excited with a pulsed laser (Nd:YAG; 355 nm) in the turning region of the reflectron field. The time-of-flight through the second drift tube section provides a mass spectrum of the selected parent ion and its photofragments, if any. The data are presented in a computer difference mode in which the dissociated fraction of the parent ion is plotted as a negative mass peak while its photofragments are plotted as positive peaks. Mass spectra are recorded with a digital oscilloscope (LeCroy) and transferred to a laboratory PC via an IEEE-488 interface.

## 3. Results and discussion

Fig. 1 shows the mass spectra measured for the iron-pyrene and iron-perylene systems. As we found previously with other metal-PAH systems [19–26], the main mass peaks detected here correspond to adducts of metal with intact PAH molecules. Apparently, these PAH species are stable enough to withstand the vaporization conditions without significant fragmentation. In the iron-pyrene system (top frame of Fig. 1), we see that clusters form with either one or two pyrene ligands and up to four iron atoms. In the iron-perylene system (bottom frame of Fig. 1), there are peaks corresponding to clusters with one and two perylene molecules with one and two iron atoms, as well as a small $Fe(per)_3^+$ peak. The most prominent mass peaks by

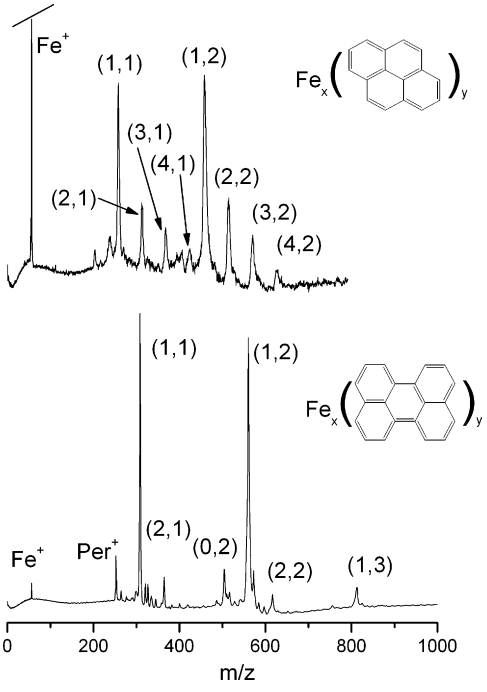


Fig. 1. The top frame shows the mass spectrum for the iron-pyrene system. The solid line at the top of this mass spectrum indicates that it has been cropped to highlight the clusters of interest, because the $Fe^+$ peak is so large. The bottom frame shows the mass spectrum for the iron-perylene system. In each spectra, the peaks labeled $(x,y)$ indicate the $Fe_x(PAH)_y$ stoichiometries for the clusters.

far for each system are those corresponding to the $Fe(PAH)^+$ and $Fe(PAH)_2^+$ ions. Smaller mass peaks correspond to multiple metal atom adducts with one or two PAH molecules. In the pyrene system, there is no evidence for isolated ions of the PAH or its dimer, while very small peaks are seen for these in the case of the perylene. The strong intensity of the 1,2 mass features for both systems and the lack of strong signals for the PAH dimers suggest that these are sandwich clusters. These systems are apparently bound together by a metal–ligand interaction that is stronger than the ligand–ligand interactions. In the iron-pyrene system, the intensities of the signals for clusters with multiple metal atoms fall off gradually with size, with up to four metal atoms seen in a cluster, whereas the most metal in any perylene cluster is only two atoms. It is therefore tempting to conclude that the binding sites or binding energies for metal are different on these two PAH species, although it is not immediately evident why this should be the case. However, this disparity may simply be an issue of the relative iron concentration in the two systems. Although we use similar conditions of film thickness and vaporization laser power, it is not possible to control the relative concentrations of metal and ligands in these systems in any detailed way. The clusters produced here are expected to depend on the detailed photophysics of the absorption process, the film desorption and metal vaporization yields, energy transfer, cluster growth and ionization processes, which may be quite different for the two PAH species.

Neither of these mass spectra exhibit any mass peaks corresponding to pure iron atom clusters that are not attached to a PAH. Iron clusters are well-known to form in environments when only metal vapor is present [49,50], but they do not form under these conditions. Apparently, the relative concentrations of ligand versus metal and the binding energies of metal to ligands is such that metal addition to ligands is more favorable than metal–metal clustering. Additionally, because no pure metal clusters are detected, the multi-metal clusters seen here have most likely formed by the addition of metal atoms one-at-a-time to these ligands. Presumably after such individual atom addition, the metals can either aggregate into clusters or bind in individual sites on the PAH surface, depending on the most favorable energetics. Except for the larger concentration of species with a single iron atom, there is no obvious preference for a special number of iron atoms. Instead, the fall-off in abundance is gradual, consistent with a decrease in the available metal concentration. A final qualitative observation is that there is no evidence for destruction of pyrene or perylene in the laser generated plasma, which could conceivably produce smaller metal-hydrocarbons or metal-carbide masses. The simple metal-ligand addition processes seen are consistent with the behavior we have documented previously for iron or chromium in complexes with coronene [19,22], but very different from that seen for niobium-PAH systems [23], where PAH decomposition was prominent.

As noted, the strong peak in each system for the $Fe(PAH)_2^+$ species suggests that these clusters exist as sandwiches. Additionally, for the clusters which have more than one metal atom, it is conceivable that these metals atoms are present as clusters on the PAH surface or as individually bound species. In order to probe these and other structural issues, we employ mass-selected photodissociation measurements.

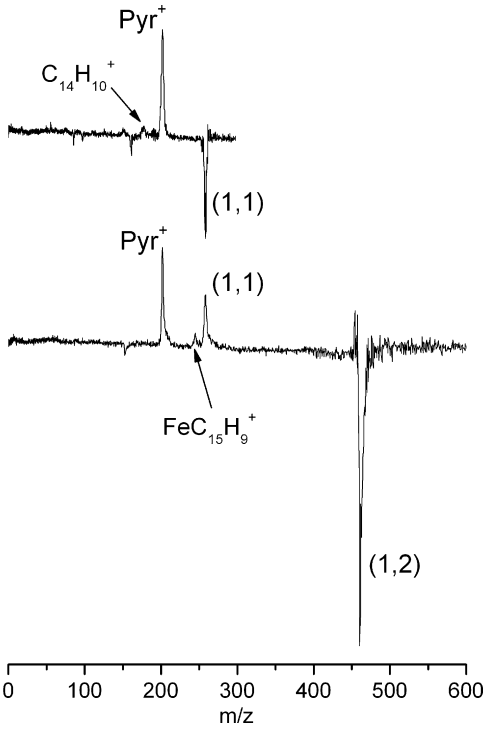


Fig. 2. The top frame shows the photodissociation spectrum of $Fe(pyr)^+$ at 355 nm. The bottom frame shows the photodissociation spectrum of $Fe(pyr)_2^+$ at 355 nm.

Fig. 2 shows the photodissociation mass spectra for the mass-selected ions of $Fe(pyr)^+$ and $Fe(pyr)_2^+$. These photodissociation spectra are collected in a computer difference mode of operation, in which the intensity of the selected ion without the dissociation laser firing is subtracted from the intensity of that ion and its fragments when the dissociation laser is firing. As a result of this procedure, the parent ion in each frame is shown as a negative peak, indicating its depletion from photodissociation, while the fragment ions at lower masses appear as positive peaks. In the top spectrum, the fragmentation of $Fe(pyr)^+$ is shown, indicating that the most prominent charged fragment is the pyrene cation. By mass conservation, it is clear that a neutral iron atom has been eliminated in the fragmentation process. The lowest energy process, and one which is seen most often in these systems, produces the fragment with the lower ionization potential (IP) as a ion, while that with the higher IP is a neutral and not detected. Although this pattern is normally followed, the fragment with the higher IP is sometimes eliminated with the charge, in a so-called charge transfer dissociation process [27,28,30]. In this system, the IP of pyrene is 7.43 eV and that of iron is 7.870 eV [51]. Therefore, the lowest energy dissociation process (i.e., one without charge transfer) would cleave the metal-ligand bond producing charged pyrene and neutral iron, and this is what we see. Additionally, there are small broad peaks detected here at $177 \pm 3$ and $151 \pm 3$ amu. Such broadened peaks are not uncommon in time-of-flight experiments, occurring from metastable fragmentation process. Mass 178 would correspond to $C_{14}H_{10}^+$, which could be the smaller PAH species

anthracene. On the other hand, a standard mass spectrum of pyrene measured with electron impact ionization has a fragment at 176 amu [52], produced by the elimination of acetylene. Either of these is a reasonable product from the continued fragmentation of the pyrene ion produced initially. However, the second peak at 151 is about 26 amu below the first, suggesting that these peaks probably indicate the sequential elimination of acetylene.

The bottom frame of Fig. 2 shows the photodissociation of the $Fe(pyr)_2^+$ cluster. The highest-mass product is $Fe(pyr)^+$, which must be formed by eliminating a neutral pyrene molecule. The most intense fragment is that of the pyrene cation. This is more than likely produced by further fragmentation of the initial $Fe(pyr)^+$ fragment. Because $Fe(pyr)^+$ is produced as an ionic fragment, it most likely has an IP lower than that of pyrene, and any pyrene produced directly from the parent ion would then be neutral. As noted above, the mass spectrum contains virtually no pure pyrene clusters. Based on this observation, we expect that the pyrene ligands have a greater attraction for the metal ion than for each other, and then this cluster would most likely have a sandwich structure. The fragmentation pattern here is consistent with this structure, and a mechanism involving the sequential loss of one ligand and then the other. However, we cannot completely rule out a metal–ligand–ligand connectivity, which might also produce the same fragmentation pattern. One other feature to note in this spectrum is a small peak corresponding to $Fe(C_{15}H_9)^+$. This fragment is apparently formed by the loss of CH from a pyrene molecule, although because of the limited resolution here we cannot rule out the additional loss of one or two more hydrogen atoms. However, it is clear that the pyrene ring system has been disrupted due to the presence of the iron atom. It would be highly unlikely for the iron atom to attach at another binding position and leave a vacancy in one of the aromatic rings. Therefore, it is likely that the iron atom has inserted into the pyrene ring system. This same type of insertion was seen previously in our study of chromium-coronene and niobium-coronene complexes [21,22], as well as in our studies of vanadium and iron with $C_{60}$ [10]. Therefore, it is perhaps understandable that a small amount of this type of fragmentation could occur with pyrene.

An interesting aspect of these systems is the production of clusters with multiple iron atoms bound to a single pyrene molecule, as well as multi-iron, multi-pyrene clusters. These types of clusters were also prominent in our previous studies of the iron-coronene and chromium-coronene systems [18,21]. As with those systems, there are two general configurations for multi-metal attachment to a pyrene molecule. The metals may disperse over the pyrene surface and bind to various ring sites via individual π or bridging interactions, as was seen in the iron-coronene system. Additionally, this type of interaction could occur on both sides of the pyrene molecule. The other possible bonding scheme is that metal atoms may aggregate together and bind as a metal cluster on the pyrene surface, as was seen in the chromium-coronene system. These various structures cannot be determined unequivocally through the use of mass spectrometry. However, we can gain some insight into these possible structures through photodissociation of these clusters.

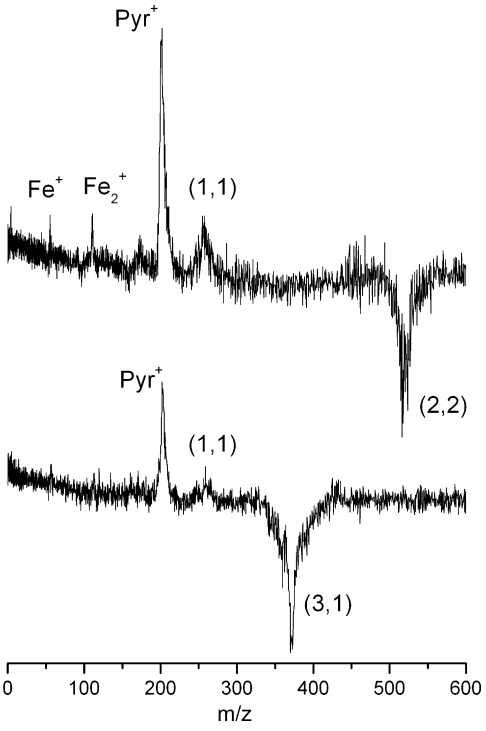


Fig. 3. Photodissociation spectra of $Fe_2(pyr)_2^+$ (top frame) and $Fe_3(pyr)^+$ (bottom frame), both at 355 nm.

The top frame of Fig. 3 shows the photodissociation spectrum of $Fe_2(pyr)_2^+$. The photodissociation spectrum of $Fe_2(pyr)^+$ (not shown) shows the same photofragments as this spectrum. The most prominent peak in both spectra is again that of the pyrene cation. Additionally, there are also less intense peaks corresponding to $Fe(pyr)^+$, $Fe_2^+$ and $Fe^+$. The presence of $Fe^+$ is surprising; because of its high IP (higher than pyrene, and then also higher than Fe(pyr)), it should be lost as a neutral and not seen as a ion. This atomic ion could come from sequential fragmentation of $Fe_2^+$, or it could come from photoionization of the neutral atom photofragments because of the intense laser light present that is intended for photodissociation. Such reionization is not uncommon in systems like these that require high laser power for fragmentation. However, it can only occur if the iron atom is ejected from the parent ion rapidly, within the 5 ns laser pulse when laser light is still present in the interaction region. The quite low IP of $Fe_2^+$ (6.30 eV) is less than that of pyrene (7.43 eV), and so this charged fragment could come from any precursor containing at least two iron atoms, but it would leave behind a corresponding neutral. This metal dimer ion therefore cannot come in a sequence from $Fe(pyr)^+$, but must come directly from either the parent ion or an intermediate $Fe_2(pyr)^+$ fragment (which is not detected). It then follows that the simultaneous observation of pyrene cation, $Fe_2^+$ and $Fe(pyr)^+$ must indicate either two parallel fragmentation channels of the same parent ion structure or the fragmentation of two different parent ion isomers.

Isomers with an alternating metal–ligand–metal–ligand structure or with two metal atoms sandwiched between two ligands are most likely. We do not expect any $Fe_2$-pyrene-pyrene$^+$ isomers because of the inefficient pyrene–pyrene binding noted

above. Of the two likely structures, it is difficult to see how the alternating species could produce any metal dimer photofragment. Likewise, if there were an alternating structure, we would expect to see some $Fe(pyr)_2^+$ as an intermediate fragment, but we do not. This 1,2 sandwich species is so abundant in the distribution from the source that it must have substantial stability, and therefore if it were generated as an intermediate at least some of it should survive to be detected. Therefore, the alternating structure does not seem likely. On the other hand, the two-atom sandwich structure for the 2,2 parent ion can explain all the fragment ions seen here. The 1,1 species could be formed by the loss of neutral pyrene followed by a neutral iron, or by the immediate loss of a neutral Fe(pyr) complex in a fission process. If the initial event is loss of neutral pyrene, then either two iron atoms or an iron dimer would be left on the remaining pyrene. The 1,1 fragment could be produced again from the loss of one of these iron atoms, or the $Fe_2^+$ species could be formed by elimination of both of these. However, because the IP of $Fe_2$ is lower than that of pyrene, any dimers desorbed would be charged, leaving a corresponding neutral pyrene. Because there is such a large combined amount of $Fe(pyr)^+$ and the pyrene ion which could come only from it, we surmise that the main dissociation channels here must be either the fission process ($2,2^+ \rightarrow 1,1 + 1,1^+ \rightarrow 0,1^+$) and/or the sequential loss of neutral pyrene and then neutral iron atom ($2,2^+ \rightarrow 2,1^+ \rightarrow 1,1^+ \rightarrow 0,1^+$). Overall, because it provides the simplest explanation of all the fragments seen, the most likely scenario is that the 2,2 parent ion is a two-metal sandwich.

Because the major ion fragments seen or implied here from the 2,2 parent have single iron atoms, and the amount of $Fe_2^+$ is small, it is tempting to conclude that this is a two-atom sandwich rather than a metal dimer sandwich. However, either atomic or diatomic fragments could conceivable come from either kind of structure. Separated atoms could form a dimer as they desorb, or a dimer could fragment during desorption. This latter scenario was suggested by Jena and co-workers in their theoretical study of $Fe_2(coronene)^+$ complexes, where they found the most stable structure to be an adsorbed iron dimer [47], even though the main photofragment from this ion was the loss of iron atoms [19]. Therefore, we cannot determine the most likely configuration for the two iron atoms in the 2,2 parent ions (or the 2,1 intermediates) here, but dimers like those suggested by Jena for the coronene complex seem plausible.

The metal dimer sandwich scenario described here for the 2,2 ion is appealing because it also explains the main details of the dissociation processes for the 2,1 and 3,1 ions. The 2,1 species (not shown) has the same photodissociation products as seen in the 2,2 spectrum shown here. This is completely consistent with its position as an intermediate in the main decomposition path of the 2,2 species. Likewise, the 3,1 ion (lower trace of Fig. 3) also has essentially the same fragments, with very small amounts of $Fe^+$ and $Fe_2^+$ barely discernable. In this case, there must be at least two iron atoms on the same side of the pyrene, but there is only slight evidence for metal dimer fragments and no evidence for the iron trimer as a photofragment. The IP of $Fe_3$ is also low (6.4 eV), and so it would be observed as an ion if it were eliminated in molecular form, but it is not detected. This again implies that the iron atoms are either bound separately on the surface, or that they are bound together but desorb separately in the dissociation process. This same kind of dissociation behavior was also seen in our previous study of $Fe_x(coronene)_y^+$ clusters [19].

The nature of the binding sites for multiple iron atoms on the pyrene surface in these complexes is of course influenced by the thermochemistry of bonding in these systems. In the growth process in our source, the temperature is elevated because of the metal vaporization process. Additionally, as metal atoms add to the organic ligands, the binding energy is released into the system. Some of this binding energy can be relaxed away by collisions, but many collisions are required for this. Because of these conditions, iron atoms adding to the pyrene surface should be mobile enough to sample many possible binding sites, and additional iron atoms can likewise sample the possibility of metal–metal binding. The binding sites with the greatest binding energy should then be produced more efficiently in the experiment. It is difficult to estimate the energetics for this system, but we have some relevant information. Armentrout and co-workers determined the bond energy of $Fe_2^+$ as 62.7 kcal/mol [50]. In competitive binding studies on iron with benzene, coronene, and $C_{60}$, our group determined that the bond energy of $Fe(coronene)^+$ is greater than that of $Fe(benzene)^+$, which is 49 kcal/mol [11]. Therefore, it is reasonable to assume that metal dimer binding here is at least comparable to the metal–ligand binding, and that adsorbed dimer structures would be reasonable energetically. Jena and co-workers have shown that a favorable configuration exists to facilitate both metal–ligand and metal–metal interactions when two iron atoms bond on the surface of coronene [47]. When these two metal atoms bind in C–C bridging sites across a ring from each other, the Fe–Fe distance is about 2.3 Å, providing effective bonding interactions. It seems reasonable that a similar configuration would be possible for pyrene or perylene.

The photodissociation of the iron-perylene system is shown in Fig. 4. The top frame of Fig. 4 shows the photodissociation spectrum of the $Fe(Per)^+$ cluster. The most prominent fragment seen is that of the perylene cation. The IP of perylene is 6.96 eV, which is lower than that of iron at 7.870 eV. Therefore, we would expect to find the loss of neutral iron with the perylene produced as a charged fragment, as seen. Also present in this spectrum is a small peak corresponding to $Fe(C_{12}H_8)^+$ and a peak representing the loss of five or six hydrogen atoms from the parent cluster. This is the only spectrum which shows any breakdown in the perylene ring structure. The loss of hydrogen is an efficient process that has been described previously in the photodissociation of PAH cations without any metal present [53].

The photodissociation spectrum for the $Fe_2(per)^+$ cluster is shown in the middle frame of Fig. 4. The main fragment peak is again the perylene cation. Also, there is a very weak signal for $Fe(per)^+$. To produce the most prominent peak of the perylene cation, the cluster must lose two iron atoms. In the same way discussed above for the pyrene complexes, iron dimer has an IP (6.3 eV) lower than that of perylene (6.96 eV), and would be eliminated as a $Fe_2^+$ cation, but individual iron atoms (IP = 7.87) can be lost as neutrals. Therefore, because no $Fe_2^+$ is observed, we can conclude that atom loss is the main process. The detec-

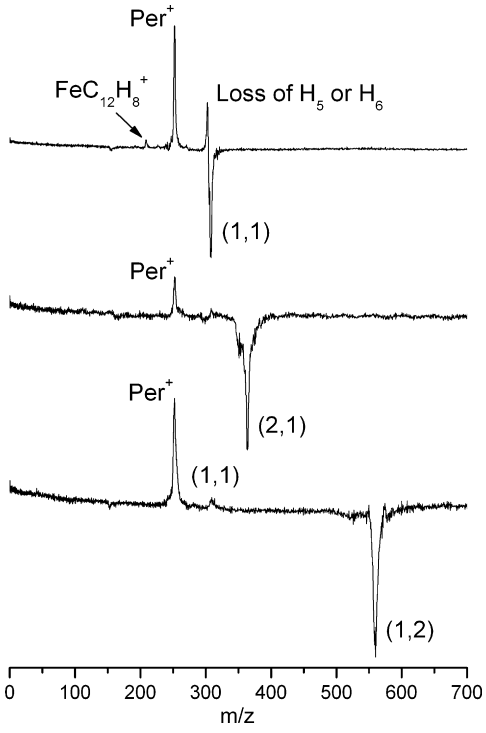


Fig. 4. The photodissociation spectra of $Fe(per)^+$ (top frame), $Fe_2(per)^+$ (middle frame), and $Fe(per)_2{}^+$ (bottom frame), all at 355 nm.

tion of $Fe(per)^+$ is completely consistent with this, as this is the expected intermediate for sequential atom loss. As we also discussed above for pyrene complexes, the loss of atoms does not allow us to conclude whether atomic or diatomic species were present initially on the PAH surface.

Finally, the bottom frame of Fig. 4 shows the photodissociation of $Fe(per)_2{}^+$. The main fragment is that of the perylene cation with a weak signal corresponding to $Fe(per)^+$. The $Fe(per)^+$ fragment is formed by eliminating a neutral perylene molecule from the cluster, while the perylene cation is likely produced by continued fragmentation of the $Fe(per)^+$. Again, as with $Fe(pyr)^+$, the presence of $Fe(per)^+$ cluster as an cationic fragment suggests that it has a lower IP than that of perylene. Moreover, since the perylene ligands would be expected to experience a greater attraction for the metal ion than for each other, this cluster most likely has a sandwich structure, as seen for the $Fe(pyr)_2{}^+$ species above.

As shown in both mass spectra and dissociation patterns, these iron-pyrene and iron-perylene cation clusters have several similarities. 1,1 and 1,2 stoichiometries are by far the most abundant for both systems. In both systems, the conditions of their formation and their dissociation patterns indicate that the 1,2 species have sandwich structures. For both PAH species, the 1,2 complex loses a neutral ligand first and then a neutral iron, consistent with sandwich structures. Likewise, the 2,2 species for iron-pyrene is most likely a two-metal sandwich. All of these systems represent clustering processes of intact PAH molecules with one or more iron atoms. The most likely growth process is sequential addition of single atoms to the PAH surface. Decomposition processes follow the reverse route; the main process seen is elimination of neutral iron atoms. In all of these characteristics, the iron-pyrene and iron-perylene systems are quite similar to the iron-coronene clusters studied previously by our group [19]. The behavior can be contrasted with chromium-coronene clusters, in which metal cluster elimination was prominent [22] or the niobium-PAH systems, where ring destruction and carbide formation were observed [23].

## 4. Conclusions

Iron cluster cations with pyrene and perylene were produced by laser vaporization and studied by fixed frequency UV photodissociation. Mass spectral data show a prominence for the $Fe(PAH)^+$ and $Fe(PAH)_2{}^+$ cluster in each system. In addition to the single metal species, multiple metal clusters are also detected. Photodissociation of all of these clusters requires high laser fluences. These conditions indicate that multiphoton absorption is required for dissociation, consistent with strong metal-PAH bonding. The dissociation patterns are consistent with sandwich structures for the 1,2 and 2,2 stoichiometry clusters. Decomposition in all of these systems is dominated by the loss of neutral metal atoms or, in the case of multi-PAH clusters, by the loss of neutral PAH species. These overall growth, bonding and dissociation properties are quite similar to those seen previously for iron-coronene clusters.

## Acknowledgement

We gratefully acknowledge the support of the Air Force Office of Scientific Research (Grant No. FA9550-06-1-0028) for this work.

## References

[1] N.J. Long, Metallocenes, Blackwell Sciences, Ltd., Oxford, 1998.
[2] T.P. Martin, N. Malinowski, U. Zimmermann, U. Naeher, H. Schaber, J. Chem. Phys. 99 (1993) 4210.
[3] U. Zimmermann, N. Malinowski, U. Naeher, S. Frank, T.P. Martin, Phys. Rev. Lett. 72 (1994) 3542.
[4] M. Springborg, S. Satpathy, N. Malinowski, U. Zimmermann, T.P. Martin, Phys. Rev. Lett. 77 (1996) 1127.
[5] F. Tast, N. Malinowski, S. Frank, M. Heinebrodt, I.M.L. Billas, T.P. Martin, Phys. Rev. Lett. 77 (1996) 3529.
[6] S. Frank, N. Malinowski, F. Tast, M. Heinebrodt, I.M.L. Billas, T.P. Martin, Z. Phys. D: At., Mol. Clusters 40 (1997) 250.
[7] F. Tast, N. Malinowski, S. Frank, M. Heinebrodt, I.M.L. Billas, T.P. Martin, Z. Phys. D: At., Mol. Clusters 40 (1997) 351.
[8] W. Branz, I.M.L. Billas, N. Malinowski, F. Tast, M. Heinebrodt, T.P. Martin, J. Chem. Phys. 109 (1998) 3425.
[9] J.E. Reddic, J.C. Robinson, M.A. Duncan, Chem. Phys. Lett. 279 (1997) 203.
[10] G.A. Grieves, J.W. Buchanan, J.E. Reddic, M.A. Duncan, Int. J. Mass Spectrom. 204 (2001) 223.
[11] J.W. Buchanan, G.A. Grieves, J.E. Reddic, M.A. Duncan, Int. J. Mass Spectrom. 182–183 (1999) 323.
[12] A. Nakajima, S. Nagao, H. Takeda, T. Kurikawa, K. Kaya, J. Chem. Phys. 107 (1997) 6491.
[13] T. Kurikawa, S. Nagao, K. Miyajima, A. Nakajima, K. Kaya, J. Phys. Chem. A 102 (1998) 1743.
[14] S. Nagao, T. Kurikawa, K. Miyajima, A. Nakajima, K. Kaya, J. Phys. Chem. A 102 (1998) 4495.

[15] S. Nagao, Y. Negishi, A. Kato, Y. Nakamura, A. Nakajima, K. Kaya, J. Phys. Chem. A 103 (1999) 8909.
[16] D.E. Clemmer, J.M. Hunter, K.B. Shelimov, M.F. Jarrold, Nature 372 (1994) 248.
[17] B.P. Pozniak, R.C. Dunbar, J. Am. Chem. Soc. 119 (1997) 10439.
[18] R.C. Dunbar, J. Phys. Chem. A 106 (2002) 9809.
[19] J.W. Buchanan, J.E. Reddic, G.A. Grieves, M.A. Duncan, J. Phys. Chem. A 102 (1998) 6390.
[20] J.W. Buchanan, G.A. Grieves, N.D. Flynn, M.A. Duncan, Int. J. Mass Spectrom. 185–187 (1999) 617.
[21] M.A. Duncan, A.M. Knight, Y. Negishi, S. Nagao, Y. Nakamura, A. Kato, A. Nakajima, K. Kaya, Chem. Phys. Lett. 309 (1999) 49.
[22] N.R. Foster, G.A. Grieves, J.W. Buchanan, N.D. Flynn, M.A. Duncan, J. Phys. Chem. A 104 (2000) 11055.
[23] N.R. Foster, J.W. Buchanan, N.D. Flynn, M.A. Duncan, Chem. Phys. Lett. 341 (2001) 476.
[24] M.A. Duncan, A.M. Knight, Y. Negishi, S. Nagao, K. Judai, A. Nakajima, K. Kaya, J. Phys. Chem. A 105 (2001) 10093.
[25] T.M. Ayers, B.C. Westlake, M.A. Duncan, J. Phys. Chem. A 108 (2004) 9805.
[26] T. Ayers, B.C. Westlake, D.V. Preda, L.T. Scott, M.A. Duncan, Organometallics 24 (2005) 4573.
[27] K.F. Willey, P.Y. Cheng, M.B. Bishop, M.A. Duncan, J. Am. Chem. Soc. 113 (1991) 4721.
[28] K.F. Willey, C.S. Yeh, D.L. Robbins, M.A. Duncan, J. Phys. Chem. 96 (1992) 9106.
[29] E.D. Pillai, K.S. Molek, M.A. Duncan, Chem. Phys. Lett. 405 (2005) 247.
[30] T.D. Jaeger, M.A. Duncan, Int. J. Mass Spectrom. 241 (2005) 165.
[31] A. Nakajima, K. Kaya, J. Phys. Chem. A 104 (2000) 176.
[32] K. Hoshino, T. Kurikawa, H. Takeda, A. Nakajima, K. Kaya, J. Phys. Chem. 99 (1995) 3053.
[33] T. Kurikawa, M. Hirano, H. Takeda, K. Yagi, K. Hoshino, A. Nakajima, K. Kaya, J. Phys. Chem. 99 (1995) 16248.
[34] T. Yasuike, A. Nakajima, S. Yabushita, K. Kaya, J. Phys. Chem. A 101 (1997) 5360.
[35] K. Judai, M. Hirano, H. Kawamata, S. Yabushita, A. Nakajima, K. Kaya, Chem. Phys. Lett. 270 (1997) 23.
[36] T. Kurikawa, H. Takeda, M. Hirano, K. Judai, T. Arita, S. Nagao, A. Nakajima, K. Kaya, Organometallics 18 (1999) 1430.
[37] S. Nagao, A. Kato, A. Nakajima, K. Kaya, J. Am. Chem. Soc. 122 (2000) 4221.
[38] T. Kurikawa, Y. Negishi, F. Hayakawa, S. Nagao, K. Miyajima, A. Nakajima, K. Kaya, J. Am. Chem. Soc. 120 (1998) 11766.
[39] T. Kurikawa, Y. Negishi, F. Hayakawa, S. Nagao, K. Miyajima, A. Nakajima, K. Kaya, Z. Phys. D: At., Mol. Clusters 9 (1999) 283.
[40] T.D. Jaeger, M.A. Duncan, J. Phys. Chem. A 108 (2004) 11296.
[41] A.C. Scott, N.R. Foster, G.A. Grieves, M.A. Duncan, Int. J. Mass Spectrom. 263 (2007) 171.
[42] A. Klotz, P. Marty, P. Boissel, G. Serra, B. Chaudret, J.P. Daudey, Astron. Astrophys. 304 (1995) 520.
[43] D.K. Bohme, Chem. Rev. 92 (1992) 1487.
[44] T. Henning, F. Salama, Science 282 (1998) 2204.
[45] J. Szczepanski, H. Wang, V. Martin, A.G.G.M. Tielens, J.R. Eyler, J. Oomens, Astrophys. J. 646 (2006) 666.
[46] R.C. Dunbar, J. Phys. Chem. A 102 (1998) 8946.
[47] S.J. Klippenstein, C.-N. Yang, Int. J. Mass Spectrom. 201 (2000) 253.
[48] L. Senapati, S.K. Nayak, B.K. Rao, P. Jena, J. Chem. Phys. 118 (2003) 8671.
[49] E.A. Rohlfing, D.M. Cox, A. Kaldor, K.H. Johnson, J. Chem. Phys. 81 (1984) 3846.
[50] S.K. Loh, D.A. Hales, L. Li, P.B. Armentrout, J. Chem. Phys. 90 (1989) 5466.
[51] S.G. Lias, in: P.J. Linstrom, W.G. Mallard (Eds.), NIST Chemistry Webbook, NIST Standard Reference Database Number 69, National Institute of Standards and Technology, Gaithersburg MD, 20899, June 2005.
[52] S.E. Stein, in: P.J. Linstrom, W.G. Mallard (Eds.), NIST Chemistry Webbook, NIST Standard Reference Database Number 69. National Institute of Standards and Technology, Gaithersburg, MD 20899, June 2005.
[53] S.P. Ekern, A.G. Marshall, J. Szczepanski, M. Vala, J. Phys. Chem. 102 (1998) 3498.